Chip integrated strategies for acoustic separation and manipulation of cells and particles

Thomas Laurell,* Filip Petersson and Andreas Nilsson

Received 29th September 2006
First published as an Advance Article on the web 7th December 2006
DOI: 10.1039/b601326k

Acoustic standing wave technology combined with microtechnology opens up new areas for the development of advanced particle and cell separating microfluidic systems. This *tutorial review* outlines the fundamental work performed on continuous flow acoustic standing wave separation of particles in macro scale systems. The transition to the microchip format is further surveyed, where both fabrication and design issues are discussed. The acoustic technology offers attractive features, such as reasonable throughput and ability to separate particles in a size domain of about tenths of micrometers to tens of micrometers. Examples of different particle separation modes enabled in microfluidic chips, utilizing standing wave technology, are described along a discussion of several potential applications in life science research and in the medical clinic. Chip integrated acoustic standing wave separation technology is still in its infancy and it can be anticipated that new laboratory standards very well may emerge from the current research.

Introduction

Spatial control and manipulation of particulate matter in fluids by means of ultrasonic standing waves is an area that is gaining increased attention. A driving factor is the simultaneous progress within microfabrication and microfluidics, which now offers methods for precision engineering of acoustic resonators as an integrated part of microfluidic networks. Ultrasonic standing wave manipulation offers a non-contact mode of particle handling, which makes it an attractive tool in cell handling microsystems as a minimum of mechanical stress is induced by the applied acoustic forces. All types of particles can be affected by ultrasonic standing wave forces as long as they differ from the surrounding medium in regards to its acoustic properties.

Acoustic standing waves were already described by Kundt[1] in the 19th century with his famous tube experiment, where cork dust was moved by an acoustic wave in a resonating air column, illustrating the standing wave pattern. Ultrasonic standing waves are generated either by the use of two opposing sound sources or more commonly by a single ultrasonic transducer which is facing a sound reflector. The ultrasonic sources commonly used are piezo ceramic elements that either are directly coupled into the liquid or *via* a coupling layer. An optional way of generating acoustic standing waves in a

Dept. Electrical Measurements, Lund University, P.O. Box 118, S-221 00, Lund, Sweden

Thomas Laurell

Thomas Laurell received his PhD degree at the Department of Electrical Measurements, Lund University in 1995 and was appointed Professor in Medical and Chemical Microsensors at the Department of Electrical Measurements, Lund University in 2000. Laurell currently leads the nanobiotechnology group at the department. His research focuses on Lab-on-a-Chip technologies for biomedical monitoring/analysis, implantable neural electrodes and micro components for liquid/cell sample handling in chemical microsystems. A strong focus is currently set on acoustic separation of particles and biological matter in microfluidic systems and the development of new nanoproteomics technology.

Filip Petersson

Filip Petersson, born in 1977, received his Master of Science degree in Engineering Physics in 2001 at Lund Institute of Technology (LTH), Sweden. He currently holds a position as PhD student in microtechnology and ultrasound physics at the Department of Electrical Measurements, LTH. His main research area is in acoustic particle separation in microfluidic systems. The research findings have resulted in several national awards, among these the SKAPA award in memory of Alfred Nobel. He is also a partner in ErySave AB, a spin-off company developing a system for blood recycling.

defined compartment is to design the resonator for a half wavelength standing wave (or a multiple thereof) whereafter the complete device is excited mechanically from an arbitrary coupling point. When subsequently tuning the excitation frequency to match the resonator compartment, a standing wave is formed. This mode of operation, coined the Lund method, was first explored by Nilsson[2] *et al.* in a continuous flow-through format for particle and cell separation.

The fundamental theory on acoustic standing wave forces on particles has been described extensively by King,[3] Yosioka and Kawasima,[4] Gorkov[5] and Nyborg[6] among others. The force induced on particles in an acoustic standing wave field is the result of both the primary and secondary radiation forces, where the primary force originates from the standing wave and the secondary forces are due to sound waves scattered by the particles. The primary radiation force (PRF) is, in general, responsible for the strongest acoustic force exerted on the suspended particles in a standing wave field. Secondary forces are commonly orders of magnitudes smaller and are only influential at very short distances between particles, *i.e.* at very high particles densities. As an example Ter Haar and Wyard[7] showed the relative magnitude of acoustic forces on red blood cells to be 2×10^{-12} N for the PRF, the secondary interparticle force to be 2×10^{-9} N for cells in contact and 10^{-14} N for cells 10 μm apart.

Theory

The primary radiation force

The primary radiation force can be divided into the axial component and the transverse component, Fig. 1. The axial PRF acts in the direction of the propagation of the acoustic wave field and is stronger than the transverse PRF.

The axial PRF translates particles or cells to either the nodes or the antinodes of the standing wave. The transverse PRF is subsequently responsible for packing the particles closer together and to withhold their positions. The equation of the axial PRF (eqn 1), states that the acoustic force is proportional to the acoustic pressure amplitude p_0 squared and to the volume of the particle V_c. As the size dependency scales with the particle volume, the cube of the radius, the induced primary force is strongly dependent on particle size and thus, as the particle diameter is reduced, the acoustic force diminishes rapidly. The acoustic contrast factor (eqn 2), represented by ϕ in eqn 1, depends on both the particle density (ρ_c) and its compressibility (β_c) in relation to the corresponding properties of the surrounding medium (ρ_w, β_w). The wave number, k, is defined by $2\pi/\lambda$ and x is the distance from a pressure node.

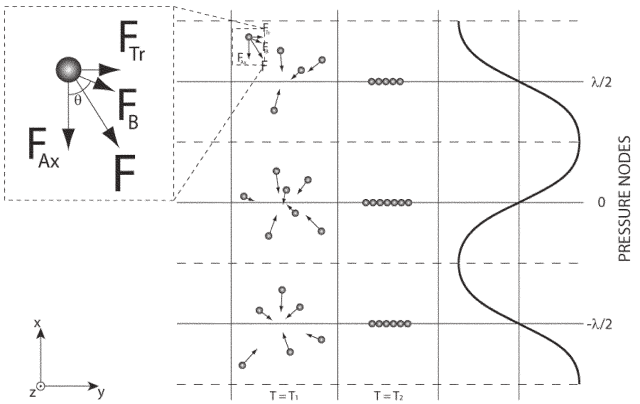

Fig. 1 Acoustic forces that act on a particle: F_{Ax} is the axial component of the primary radiation force, F_{Tr} is the transverse component and F_B are the interparticle forces (Bjerknes forces). At time T_1 the acoustic forces have just begun to act on the particles and by time T_2 a steady state has been reached.

$$F_r = -\left(\frac{\pi p_0^2 V_c \beta_w}{2\lambda}\right)\cdot\phi(\beta,\rho)\cdot\sin(2kx) \quad (1)$$

$$\phi(\beta,\rho) = \frac{5\rho_c - 2\rho_w}{2\rho_c + \rho_w} - \frac{\beta_c}{\beta_w} \quad (2)$$

A most notable aspect of the acoustic contrast factor is the possible sign change depending on the densities and compressibilities, which determines the direction of the acoustic force and thus whether the particle will move towards the standing wave pressure node or the antinode. Generally, solid particles in aqueous media are moved towards a pressure node while *e.g.* gas bubbles are moved towards the pressure antinode. Because of the acoustic contrast factor, even particles which are neutrally buoyant can experience an acoustic force as long as the compressibility differs from the surrounding medium. The pressure amplitude in eqn 1 is proportional to the supplied voltage when actuating with a piezoelectric ceramic.[8]

Secondary acoustic forces

When multiple particles in a suspension are exposed to a standing wave field, they will not only experience the primary acoustic force, but also the secondary forces caused by waves scattered by other particles. The interparticle forces are sometimes called Bjerknes forces, after the pioneering work by Bjerknes.[9] A simplified equation for the interparticle forces (eqn 3), when the acoustic wavelength is much greater than the particle radius and the distance between the particles, was derived by Weiser *et al.*[10] This work was based on results from Crum,[11] which showed that it is possible to superposition the

Andreas Nilsson

Andreas Nilsson received his Master of Science in Electrical Engineering at Lund Institute of Technology in 2002. He is currently a PhD student at the department of Electrical Measurement in Lund and his research is mainly focused on acoustic particle and cell manipulation in microfluidic channels. He has received several national innovation awards including the SKAPA award 2003. He is currently involved in ErySave AB, a spin-off company commercializing acoustic blood-washing technology.

equation for the force on a rigid sphere with the corresponding force for a compressible sphere.

$$F_B(x) = 4\pi a^6 \left[\frac{(\rho_c - \rho_w)^2 (3\cos^2\theta - 1)}{6\rho_w d^4} v^2(x) - \frac{\omega^2 \rho_w (\beta_c - \beta_w)^2}{9d^2} p^2(x) \right] \quad (3)$$

In eqn 3, a is the radius of the particle, d is the distance between the particles and θ is the angle between the centre line of the particles and the direction of propagation of the incident acoustic wave. The sign of the force is to be interpreted such that a negative sign means an attractive interparticle force and a positive sign means a repulsive force. The left side of the equation depends on the particle velocity amplitude $v(x)$ and the right side depends on the acoustic pressure amplitude $p(x)$. When particles are lined up in the direction of the acoustic wave propagation (θ = 0°) the velocity-dependent term is repulsive, and likewise attractive when the particles are perpendicular (θ = 90°) to the incident wave propagation. The pressure-dependent term is not affected by particle orientation at all and is always attractive. It is notable that the velocity-dependent term diminishes as particles are driven to the velocity node (pressure antinode), as in the case of air bubbles and lipid vesicles. In a similar way the pressure-dependent term diminishes as particles are driven towards the pressure node (velocity antinode), as are most solid particles in aqueous solutions. The influence of the secondary forces is usually very weak, due to the distance term d in the denominator, which means that it is only effective when the distance between particles is very small. The secondary force becomes important in aggregation and sedimentation applications, where particles initially are gathered in nodes by the PRF, and as interparticle distances become smaller the secondary forces assist in a further aggregation until the clusters finally become heavy enough for the gravity to overcome the buoyancy and start the sedimentation process.

Acoustic resonator modelling

Building the ideal acoustic resonator has proven to be a complex task. Much care must be taken in designing and assembling the different parts of the resonator in such a way that an optimal coupling of acoustic energy into the fluid chamber is obtained. Extensive modelling and research on designing acoustic resonator systems have been reported. Groschl[12] describe the acoustic system performance in layered resonators, starting from the electrical properties of the piezoelectric actuator, including the coupling layers, and finally to the generated acoustic field quantities of the resonator. Further acoustic resonator model developments have provided advisory design criteria in regards to selecting the thickness in terms of $\lambda/2$ and $\lambda/4$ for a) the acoustic coupling layer, b) the fluid layer and c) the reflector. The numerous configurations presented predict the position of the pressure node in the fluid chamber and also indicate the obtained acoustic energy density therein.[13] More recent model developments have provided the ability to place the pressure nodal plane at different positions in the resonator by tuning the excitation frequency. The model also takes into account the phenomenon of frequency splitting, *i.e.* when the dimension of the resonator chamber is matched to the transducers resonance frequency.[14] In this case the system resonance occurs at two frequencies, one lower and one higher than the original $\lambda/2$ criterion of the fluid chamber. Further modelling of resonators operated close to the frequency splitting criterion, also denoted coincidence resonance, emphasises the system sensitivity to small changes in resonator design.[15]

Macro scale acoustic standing wave particle manipulation

To a large extent, previous work on acoustic standing wave manipulation of particle suspensions has targeted batch volume systems or fluidised bed systems rather than microfluidic systems. One extensively researched topic is to utilize acoustic standing waves to aggregate cells in clusters whereby sedimentation takes place. Limaye[16] *et al.* used a circular transducer at the end of a tube containing suspended particles (yeast or *Escherichia coli* bacteria). Initially the ultrasound was applied continuously while the cells lined up in periodic aggregates, $\lambda/2$ apart, along the central axis in the tube. This was followed by a period of pulsed ultrasound, allowing the cells to sediment and the clarified supernatant was then removed from the top. Cousins[17] *et al.* used a similar model comprising a glass tube and a circular ultrasonic transducer system to separate plasma from whole blood. The glass tube contained 4 ml whole blood which was sonicated. The PRF concentrated the red cells to a level where secondary forces caused the cells to aggregate more strongly, making them too heavy to sustain their buoyant position and thus inducing sedimentation. Blood separation by aggregation and sedimentation was also done by Peterson[18] *et al.* They used a continuous system where blood entering a chamber from the bottom was exposed to a travelling wave, which forced the red blood cells from one side of the chamber to the other, where aggregation and sedimentation took place. The enriched erythrocytes were removed at an outlet parallel to the inlet and the clarified plasma was removed from the top. A similar design was used by Hawkes and Coakley,[19] who used the device to concentrate yeast suspensions.

Both Groschl *et al.*,[20] Trampler *et al.*[21] and Pui *et al.*[22] have used the aggregation and sedimentation technique in a cell culture fermentation device. Hybridoma cells were used in a bioreactor and fed with nutrient solution. Antibody-rich solution was harvested through an outlet channel which included an ultrasonic trap. The hybridoma cells were forced together in the ultrasonic standing wave field and sedimented back into the bioreactor and thus eliminating a loss of cells in the harvesting procedure.

The aggregation and sedimentation techniques are all dependent on gravity to work. Continuous separators with flow splitters are not burdened by this. An h-shaped separator was presented by Benes[23] *et al.* where particles were focused in plane with the inlet channel in a multi node standing wave. The flow channel was expanded and divided into two outlets downstream. By balancing the outlet flows, across a flow splitter, a clear medium was withdrawn at the outlet closest to the transducer and the particle suspension was collected at the

outlet furthest away from the transducer. The h-shape separator has also been tested in microgravity proving that it works well without the presence of gravity.[24] Particle extraction efficiencies of 91–97% were reported at flow rates of 14 l per day, with 48% of the flow exiting through the enriched flow outlet.

Gupta[25,26] *et al.* and Grossner[27] *et al.* used a flow chamber filled with a porous medium. Unconsolidated glass bead beds, aluminium meshes and polymeric foam were used as a porous stationary phase. As the suspended particles passed through the porous medium, secondary forces were believed to cause the particles to stick onto the surface of the porous medium. The particles were trapped in the medium as long as the ultrasound was active. When the ultrasound was switched off, the particles were released and washed away. The limitation of this system is that the porous mesh will eventually become saturated and the separation efficiency will drop. This porous medium ultrasonic separator has also been used to separate oil droplets from aqueous emulsions.[28]

Continuous separation of suspended particles utilizing flow splitters in combination with a laminar flow has also been described. The acoustic standing wave will cause a band or multiple bands of particles to form according to the position of the nodes or antinodes in the flow-through resonator.[29,30] By proper flow balancing of the outlets and the spatial positioning of the standing wave, a band of particles can be directed into a selected channel while a cleared medium is collected in other channels. This mode of operation represents an attractive way of implementing acoustically controlled continuous flow separators. Different types of flow splitters have been used. Yasuda *et al.* used a capillary inserted in their separation chamber to act as a flow splitter to collect the separated particles.[31]

Fractionation of suspended particles in a standing wave field utilizing the fact that particles with dissimilar size or physical properties are affected differently by the radiation force has also been reported by several groups. Larger particles will for example experience a larger acoustic radiation force than smaller ones, which means that they will move faster to a node or an antinode than the smaller ones. By the use of flow splitters at the outlet and balanced flows it is possible to separate the large particles from the smaller ones since they have travelled different distances.[32–34]

It is also possible to separate particles of the same size if they have different compressibility or density, thus defining each particle type by its unique acoustic contrast factor Φ. Gupta[35] *et al.* demonstrated that this separation was possible if the carrier medium was balanced in such a way that the acoustic contrast factors of the two particle types were of different signs. This mode of particle separation follows a binary clustering of particles having either positive or negative acoustic contrast factors. In order to obtain a higher degree of differentiation, sequential steps of media balancing and acoustic separation are required.

A further iteration on particle sizing was proposed by Mandralis[36] *et al.* who used a combination of frequency switching of higher harmonics with flow cycle switching. Mandralis utilized the fact that smaller particles move considerably slower in an acoustic standing wave field than a corresponding larger particle. If this fact is implemented in a laminar flow profile, particles that move fast into the high flow rate zone are also shifted a longer distance along the flow direction as compared to smaller particles in the same period of time. If subsequently the acoustic excitation is shifted to the first harmonic of the resonator, two nodes are formed, withdrawing particles from the centre and the high flow rate regime of the channel. By altering the acoustic driving conditions between the fundamental resonance and the first harmonic, synchronised with an oscillating parabolic flow, a net transport of particles exceeding a defined size will be enriched towards one end of the fluidic system and the smaller particles are concentrated at the other end of the separation device. This principle was also demonstrated to work in a continuous separation mode.

Microscale acoustic standing wave particle manipulation

An advantage of working in the microscale domain is that the flow is predominantly laminar, making flow splitter based fractionation systems efficient in continuous flow particle separation. Microscale is also beneficial when utilizing acoustic standing waves to manipulate particles as smaller channels and thus reduced resonator dimensions inherently lead to higher resonance frequencies. This in turn yields stronger radiation forces on the particles since the primary radiation force is proportional to the frequency and thus a stronger particle focusing and consequently a better separation performance. On the other hand as the particles become smaller the primary radiation force is rapidly decreased. The particle sizes that commonly allow manipulation by the primary radiation force range between a few tenths of micrometers to tens of micrometers when considering aqueous based solutions (speed of sound ≈ 1500 m s^{-1}). In that case, the upper size limit is set by practical aspects such as sedimentation or channel blocking. Also, the fact that as the channel size approaches the upper size limit the primary radiation force becomes too weak to offer a stable separation performance. Typical channel dimensions in the standing wave direction range from a millimetre to a few tens of micrometers, which approximately corresponds to an operating frequency in the 100 kHz to the 10 MHz range. These effective operating domains indicate that the microscale is a preferred dimensional regime to design acoustic separation systems. Further benefits of the miniaturisation of acoustic microfluidic separator systems is the ease of integration with more advanced microfluidic networks and downstream analytical components, accomplishing complete lab-on-a-chip systems for microparticle, *e.g.* bead or cell based, analysis and separation.

Microfluidic acoustic separators have been developed by several groups in the recent years. Hawkes[30] *et al.* presented a microfluidic separation device realized in stainless steel by wire electro discharge machining followed by fine polishing of the acoustic surfaces. The separator was realised both in the form of an h-separator as outlined by Benes[23] and as a Y-shaped separator similar to the design reported by Nilsson *et al*. In contrast Nilsson[37] *et al.* demonstrated a continuous particle concentration device based on wet etched silicon and a bonded

glass lid to create the separation channels. The ultrasonic transducer was applied underneath the channel, utilizing the propagation mode conversion of the sound wave to create a standing wave field in the flow channel orthogonal to the incident acoustic excitation. Harris *et al.* used both anisotropically wet etched silicon and isotropically etched glass to create a separation device which comprised a single inlet through a silicon chip and a flow-through cavity, etched in an opposing glass chip. The glass recess had smoothly curved sidewalls due to the isotropic etch and was not suitable for standing wave formation in this direction. However, the bottom of the recess was flat and served well as acoustic reflector, forming a resonator between the transducer surface and the glass recess and focusing the incoming particles into a sheet. The device had two outlets *via* the silicon chip, enabling the balancing of the outlet flows such that the particle enriched fraction excited *via* one of the outlets and the clear fraction through the other.[38–40] In these papers the acoustic properties of the device were both measured and modelled. Kapishnikov[34] *et al.* demonstrated a microfluidic acoustic separator realised by photolithography in SU-8, where particle sizing was accomplished by utilizing the particle specific migration velocities across the flow channel. The channel was terminated by a flow splitter to collect particles in two different size fractions.

Lilliehorn[41] *et al.* described a microsystem that used SU-8 photolithography defined microchannels on a glass plate. The SU-8/glass flow channel was clamped onto a printed circuit board holding integrated miniature piezoceramic transducers, forming local acoustic resonator zones in the flow channel. Each resonator zone generated a pressure node in the centre of the flow channel, which could trap and enrich particles and cells in a continuous flow system. Lilliehorn[42] also presented a paper where the ultrasonic trapping microarray was used to trap microbeads in zones accessible for different fluids *via* multiple microchannels connected to the trapping zone. Thereby a non-contact and continuous flow bioassaying system utilizing *e.g.* antibody-activated microbeads was enabled. Wiklund[43] demonstrated a fused silica capillary integrated with an acoustic standing wave resonator in the capillary length direction. This configuration enabled trapping of microparticles in several standing wave nodes along the capillary. Particle size selection was also performed by matching Stokes drag force to the trapping force, which scales with the volume of the particle. In a different configuration Wiklund[44] *et al.* also used ultrasonic standing waves to trap and concentrate cells in single-layer aggregates at well defined positions in a 96-well microtitre plate format for high sensitivity bioanalysis utilizing confocal fluorescence microscopy. Confocal fluorescence detection of acoustically concentrated and aggregated beads for human thyroid hormone assaying was reported at a limit of detection of 20 fM.

Designing microfluidic acoustic resonators

When designing an acoustic resonator for suspended particle separations the choice of construction material is of major importance. A key aspect concerns the accomplishment of a mechanical system that efficiently transmits the acoustic power from the piezo ceramic device into the fluid filled resonator chamber. This is commonly done *via* a matching layer of a suitable material. A clear option in coupling the acoustic signal into the fluidic system is to design the resonator in such a way that one of the walls between which the acoustic standing wave is induced is the actual acoustic actuator.[41] Iterations of this design include either two opposing transducers that are phase matched to position the acoustic pressure node at a certain position in the resonance chamber[34] and the Lund method (further described below) where a resonator chamber is excited mechanically from an arbitrary position at a frequency that corresponds to $n^*\lambda/2$ of the resonator width. The choice of material in all the above cases favours the use of high Q-value materials, *i.e.* materials that transmit sound waves at low losses. The material should also display good acoustic reflection properties when the sound wave transits from the fluidic media (usually aqueous) into the boundary wall (reflection). Low acoustic losses in the bulk material inherently also offer a low temperature rise which otherwise may be a problem if increased acoustic power input is needed.

In this perspective silicon has proven a well suited material. Table 1 provides material property data for some potential material choices where the compressibility and Young's modulus are good indicators on suitable materials. It can also be commented that silicon displays good thermal conductivity properties. Based on the given material data glass also turns out as a good candidate material in resonator constructions. Since glass and silicon are a frequently used material combination in microfabrication, a close to ideal material match is found for the design of microfluidic based acoustic separation systems. PMMA and PC are less suitable in acoustic resonators but are listed for comparison.

The favourable microfabrication properties of silicon also make it the material of choice. A fundamental requirement in the design of a good resonator is that the two opposing reflector surfaces are truly parallel in order to obtain a good acoustic standing wave. The monocrystalline properties of industrial silicon wafers further assist in the design of ideal acoustic reflector walls. As monocrystalline silicon is available in cuts of various crystal orientations, *e.g.* ⟨110⟩ and ⟨100⟩, as defined by their Miller indices, a multitude of design options are available (Fig. 2). The crystal orientation is of importance when fabrication processes based on standard anisotropic wet etching are used. If deep reactive ion etching (DRIE) is employed to fabricate vertical channel walls as acoustic reflector surfaces, wafer crystal orientation is of no importance. It can, however, be pointed out that the tolerance requirements when employing the DRIE-process to fabricate acoustic resonators are highly critical in regards to reflector

Table 1 Physical material properties of some materials used in acoustic resonator designs

	Density/ kg m^{-3}	Compressibility/ Pa^{-1}	Speed of sound/m s^{-1}	Young's modulus/GPa
Silicon	2330	6,0E-12	8430	130
Steel	7900	3,8E-12	5790	200
Pyrex glass	2330	1,4E-12	5500	63
PMMA	1150	1,3E-12	2590	3
PC	1200	1,8E-10	2160	2

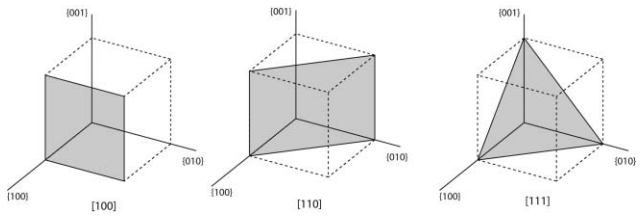

Fig. 2 Fundamental crystal planes of monocrystalline silicon and their respective Miller indices.

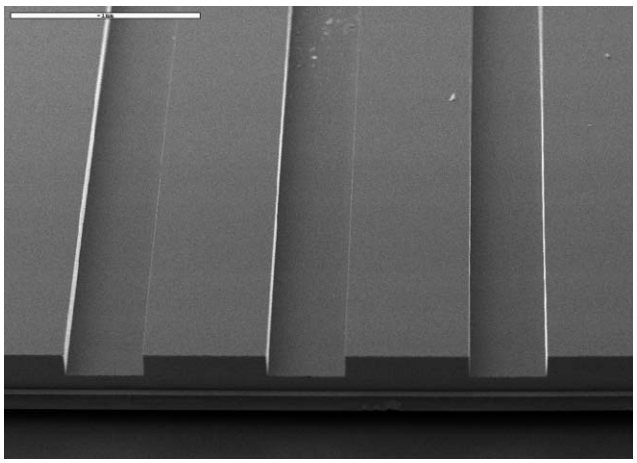

Fig. 3 A SEM showing the ideal vertical and parallel opposing channel walls when silicon is anisotropically etched. The perfect vertical walls are ideal for standing wave acoustics.

wall aspect ratio. It is therefore recommended that conventional anisotropic wet etching is performed when resonator designs are made that include two opposing reflector walls in the bulk silicon material, which is the case for systems based on the Lund-method. Fig. 3 shows three parallel anisotropically etched microchannels, in an ⟨100⟩-oriented wafer, with perfectly flat and parallel side-walls. The side walls also define slow etch directions, when using KOH as the etchant. The fundamental processes for performing the microfabrication and manufacturing of acoustic resonator flow channels are more extensively outlined in the literature.[45]

When actuating a well designed resonator channel at its fundamental resonance frequency the particles will be focused in a single pressure node, forming a confined streaming band of concentrated particles in the centre with particle free

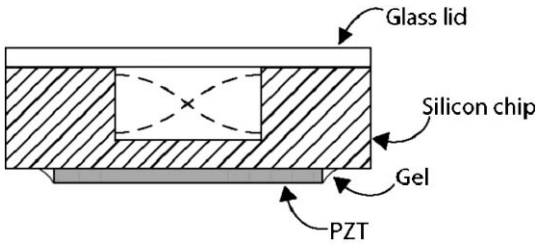

Fig. 5 Schematic cross-section of separation chip utilizing the Lund method. The silicon separation channel is sealed by a boron silica glass lid and is actuated from below using a piezoelectric ceramic.

medium at the sides. By providing the end of the resonator channel with a flow splitter, a trifurcation outlet, the focused particle stream can be collected in the centre outlet and the clear fluid can be collected at the side outlets of the flow system. Anisotropic wet etching provides several options in designing the trifurcation outlet. The most straightforward approach is to etch the side outlets at 90° to the separation channel, Fig. 4a, obtaining identical lateral etch conditions as for the resonator channel. A more optimal flow splitter design with respect to the fluid dynamics is the Y-design, where the side channels are at a 45° angle *versus* the resonator channel, Fig. 4b. A yet more intriguing flow splitter design obtained by KOH wet etching is seen in Fig. 4c. This design was realised in ⟨110⟩-oriented silicon. Although ⟨110⟩-silicon is less frequently used this crystal orientation offers a space saving design if large scale parallelisation on a wafer is to be realised.

Acoustic particle manipulation in microfluidic silicon devices

Acoustic particle focusing and separation

The Lund-method for acoustic separation of suspended particles from their medium is based on a laminar flow microchannel that is ultrasonically actuated from below, using a piezoelectric ceramic (Fig. 5).[37] The width of the channel is chosen to correspond to half the ultrasonic wavelength, thereby creating a resonator between the side walls of the flow channel in which a standing wave can be formed. The induced standing wave is thus generated orthogonal to the incident ultrasonic wave front. As suspended particles with a positive ϕ-factor perfuse the channel they are moved, by means of the axial PRF, towards the pressure nodal plane

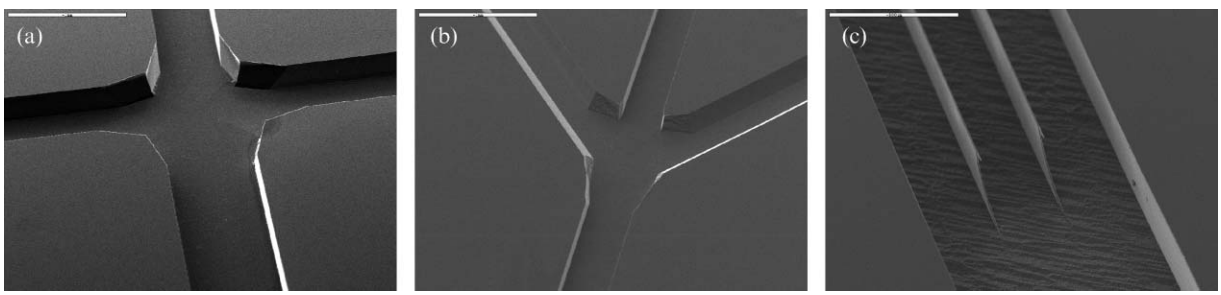

Fig. 4 a: Silicon flow channel with 90° flow splitters etched on a ⟨100⟩-oriented silicon wafer. b: Silicon flow channel with 45° flow splitters etched on a ⟨100⟩-oriented silicon wafer. c: Silicon flow channel with straight flow splitters etched on a ⟨110⟩-oriented silicon wafer.

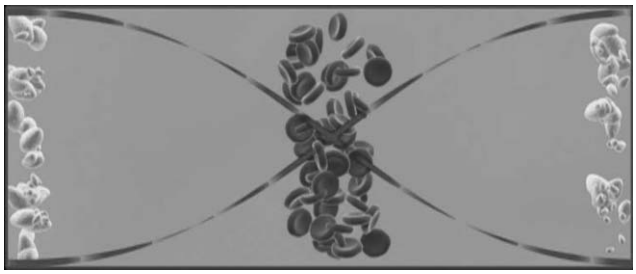

Fig. 6 Illustrated cross-section (along the dashed line in Fig. 7) of a separation channel showing negative ϕ-factor particles (*e.g.* lipid particles) collected in the pressure antinodes by the side walls and positive ϕ-factor particles (*i.e.* red blood cells) in the pressure node.

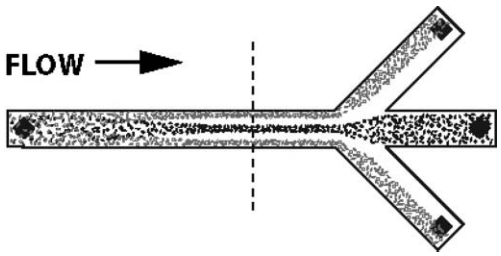

Fig. 7 Illustration of separation of negative ϕ-factor particles (black – centre outlet) and positive ϕ-factor particles (grey – side outlets) in 45° design chip.

along the channel centre, while those with a negative ϕ-factor are moved towards the anti-nodal planes close to the side walls (Fig. 6).[46] The end of the separation channel is split into three outlet channels, thus allowing the positive ϕ-factor particles to exit through the centre outlet and the negative ϕ-factor particles to exit through the side outlets, provided that all outlet flow rates are alike (Fig. 7). The separation efficiency of positive and negative ϕ-factor particles is defined as the fraction of particles exiting through the centre and side outlets respectively.

Early chip designs comprised a simple cross-structure etched on a ⟨100⟩-oriented silicon wafer where the separation channel walls were {100}-planes (Fig. 8(I)).[37] Conventional anisotropic etching thereby provided absolutely vertical side walls for the

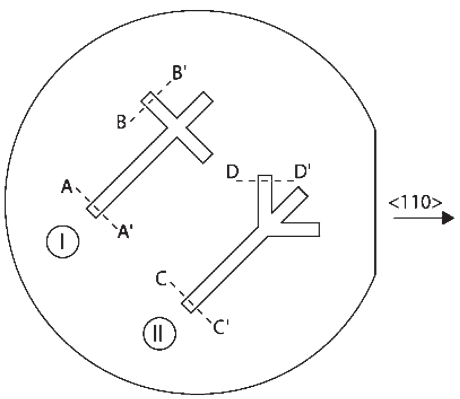

Fig. 8 Orientation of 90° (I) and 45° (II) designs on a ⟨100⟩-oriented silicon wafer. The cross-sections A, B and C are rectangular whilst D is trapezoid.

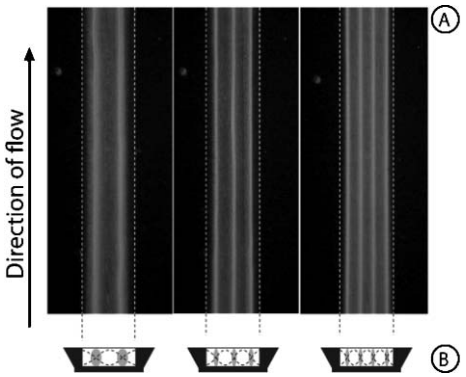

Fig. 9 Microscope image of 5 μm polyamide particles aligned in parallel bands in a ~750 μm wide channel at different actuation frequencies. left: first harmonic (~2 MHz), middle: second harmonic (~3 MHz), right: third harmonic (~4 MHz), microscope image from above (A), illustrated cross-section (B).

acoustic resonator channel. The separation channel was ~750 μm wide and ~250 μm deep, the prior dimension corresponded to the fundamental resonance frequency, *i.e.* ~1 MHz in water. In operation, the axial PRF was found to be too weak to efficiently move 5 μm polyamide spheres (positive ϕ-factor) to the middle of the channel. To increase the axial PRF the frequency was doubled (~2 MHz), *i.e.* the first harmonic was used. This resulted in a single wavelength standing wave between the side walls (Fig. 9 left). At ~2 MHz the polyamide particles gathered in the pressure nodal planes one quarter of the channel width from each side wall and subsequently exited the system through the side outlets, when the flow rates in all outlets were identical. Stagnant zones were observed in the early chip designs with outlets diverging 90° from the main channel (Fig. 10). A second design offering more harmonic fluid dynamics comprised side outlet channels diverging only 45° from the main channel direction (Fig. 8(II) and 11). Using this chip design ~90% of the suspended particles were collected in 2/3 of the original medium volume[37] (total flow rate: 0.1 ml min^{-1}, actuation frequency: ~2 MHz,

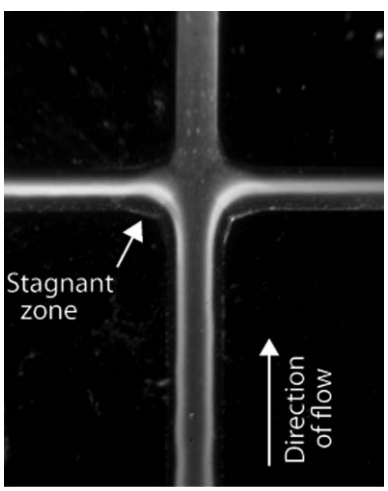

Fig. 10 Microscope image of 5 μm polyamide particles exiting a 90° design chip through the side outlets (first harmonic, ~2 MHz). Note the stagnant zones.

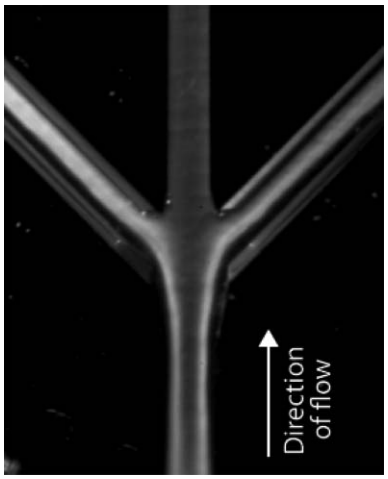

Fig. 11 Microscope image of 5 μm polyamide particles exiting a 45° design chip through the side outlets (first harmonic, ~2 MHz).

actuation voltage: 15 V_{pp} (peak-to-peak), particle concentration: 2% by volume).

Since the ~2 MHz axial PRF was sufficient to move 5 μm polyamide particles, a chip design with the corresponding fundamental resonance frequency was fabricated.[46] In this design, the channel width was ~350 μm (depth ~125 μm), corresponding to half a wavelength at ~2 MHz. Consequently, the polyamide particles now exited through the centre outlet while most of the suspending medium exited through the side outlets, provided that the flow rates in all outlets were identical. When the voltage applied to the piezoelectric ceramic was increased, the acoustic force also increased and the particles were gathered in a narrower band. At 12 V virtually all particles exited through the centre outlet together with 1/3 of the suspending medium (Fig. 12, total flow rate: 0.3 ml min^{-1}, actuation frequency: ~2 MHz, actuation voltage: 12 V_{pp}, particle concentration: 2% by volume). The maximum applicable voltage was determined by the heating of

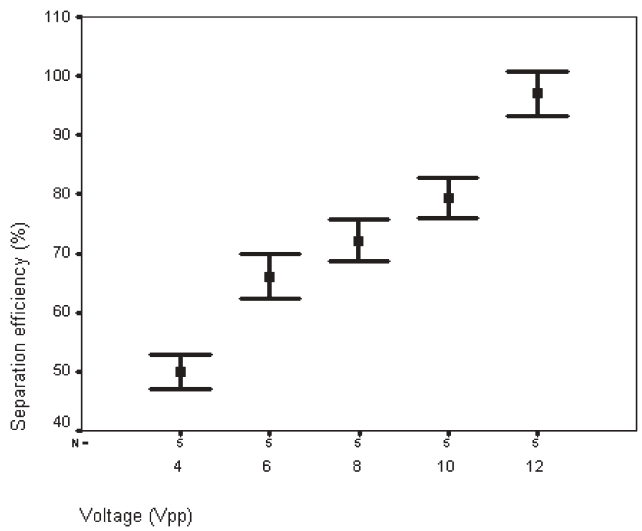

Fig. 12 Separation efficiency of the 350 μm design *versus* voltage applied to the piezo ceramic (total flow rate: 0.3 ml min^{-1}, actuation frequency: ~2 MHz, particle concentration: 2% by volume).

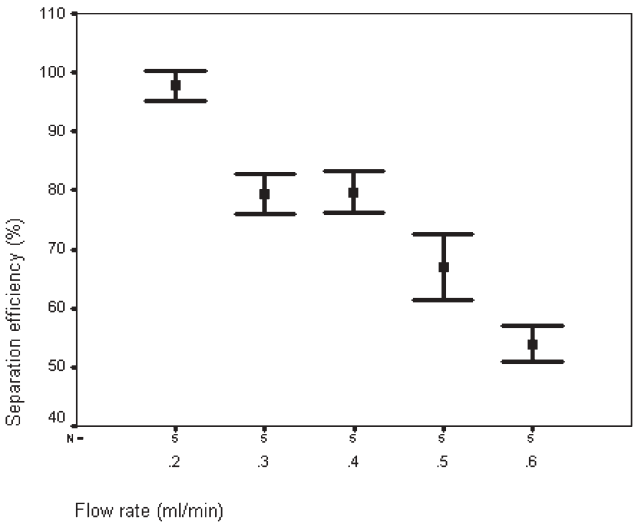

Fig. 13 Separation efficiency of the 350 μm design *versus* total flow rate (actuation voltage: 10 V_{pp} actuation frequency: ~2 MHz, particle concentration: 2% by volume).

the chip due to losses in the actuator and by trapping of particles in the flow channel, the latter most likely a result of the transverse PRF.[47] If the flow rate was increased the particle band became wider since the particles resided in the standing-wave field for a shorter period of time, resulting in a reduced separation efficiency (Fig. 13). A higher concentration of suspended particles also had a negative effect on the separation efficiency since more particles demanded a stronger acoustic force and because the centre outlet was overloaded (Fig. 14).

One of the first applications of the acoustic separation method targeted blood washing in open-heart surgery.[46,48,49] In general, blood shed in the chest cavity during surgery, *e.g.* coronary bypass, is collected and returned to the patient *via* a filter. This blood is commonly contaminated by triglycerides

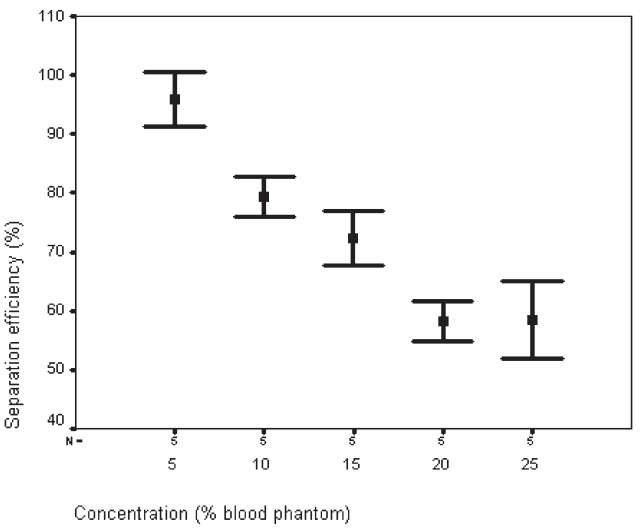

Fig. 14 Separation efficiency of the 350 μm design *versus* blood phantom concentration (total flow rate: 0.3 ml min^{-1}, actuation voltage: 10 V_{pp}, actuation frequency: ~2 MHz). A 10% blood phantom concentration corresponds to a 2% particles concentration by volume.

from adipose tissue undergoing surgery. However, when autotransfusion is performed, millions of small lipid particles (lipid microemboli) pass straight through the filter and are introduced into the patient's circulatory system, resulting in microembolisation of the capillary network in the bodily organs and subsequent local ischemic tissue damage. This becomes most obvious with regard to the brain.[50] Elevated levels of cognitive dysfunction have been linked to lipid microembolisation of the brain.[51] No dedicated methods to remove lipid microemboli are currently available. Autotransfusion is clearly preferred in spite of the aspects of microembolisation since returning the patient's own blood reduces the strain on the blood banks. In addition, it eliminates transfusion transmitted disease, immunologic reactions and the risk of blood group incompatibility. In the case of extensive blood loss, blood wash devices based on centrifuges can be used. These are, however, burdened with a number of drawbacks. They can only handle large volumes of blood, they expose the blood cells to harmful mechanical stress (high g-levels) and are non continuous. Fortunately, lipid particles display a negative ϕ-factor (~ -0.3) while being positive for erythrocytes ($\phi \approx \sim 0.3$). This means that, while passing through a $\sim$350 μm wide separation channel actuated at $\sim$2 MHz, lipid particles will move towards the side walls and exit the system *via* the side outlets while erythrocytes move to the centre and exit through the centre outlet (Fig. 15). The fraction of the suspending medium that exits the system together with the lipid particles will be determined by the flow speeds set for the different outlets.

In a study on lipid microemboli separation, a sonicated emulsion of tritium-labeled trioleine in saline solution was used to evaluate the lipid particle separation efficiency. The measurements were performed by detecting the radioactivity of the waste and enrichment fractions. It was shown that about 85% of the lipid particles were removed independent of the concentration of erythrocytes, while the erythrocyte recovery decreased at elevated hematocrit levels (Fig. 16 and 17, total flow rate: 0.3 ml min^{-1}, actuation frequency: $\sim$2 MHz, actuation voltage: 10 V_{pp}, erythrocyte concentration: 2.5–10.0% by volume, lipid concentration: 1% by volume).[46] The

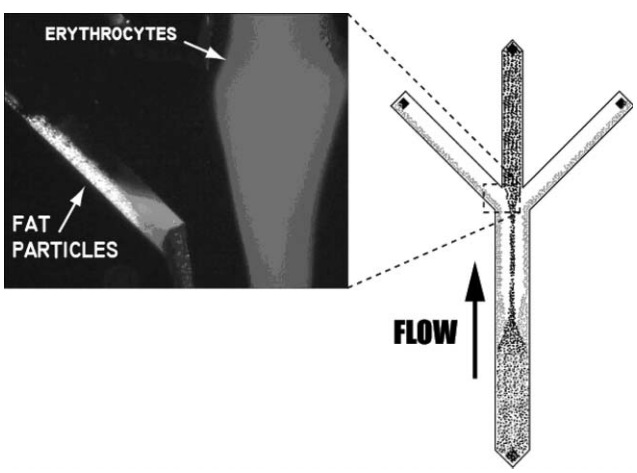

Fig. 15 Microscope image showing human lipid (fat) particles being separated from red blood cells (erythrocytes).

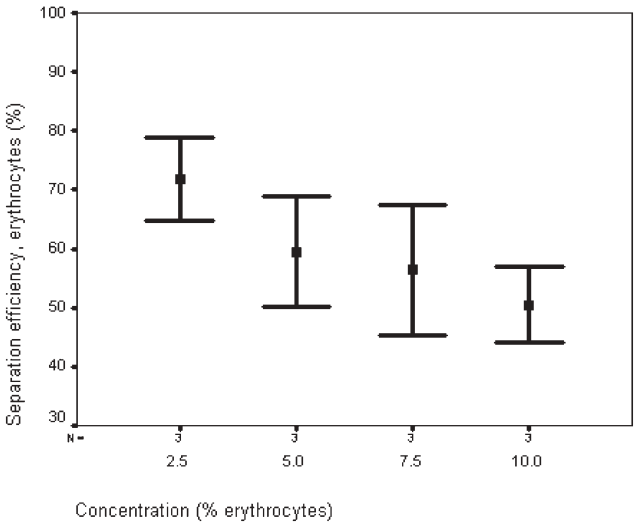

Fig. 16 Erythrocyte separation efficiency *versus* erythrocyte concentration (total flow rate: 0.3 ml min^{-1}, actuation frequency: $\sim$2 MHz, actuation voltage: 10 V_{pp}, lipid concentration: 1% by volume).

concept of increasing the throughput by using several parallel channels was later demonstrated (Fig. 18). The mean separation efficiency, for both erythrocytes and lipid particles, was found to be around 80% in the investigated concentration range (5–30% erythrocytes and 0.5–2.0% lipid particles by volume, eight parallel channels, centre outlet flow rate: 0.5 ml min^{-1}, total side outlet flow rate: 0.5 ml min^{-1}, actuation frequency: $\sim$2 MHz, actuation voltage: 18–28 V_{pp}).[48] A parameter to take into account regarding the erythrocyte separation efficiency is overloading of the centre outlet at higher hematocrit levels. The first step in improving the characteristics comprises balancing of the waste and enrichment flow rates. The implementation of serially linked separation channels can further improve the situation. Fig. 19

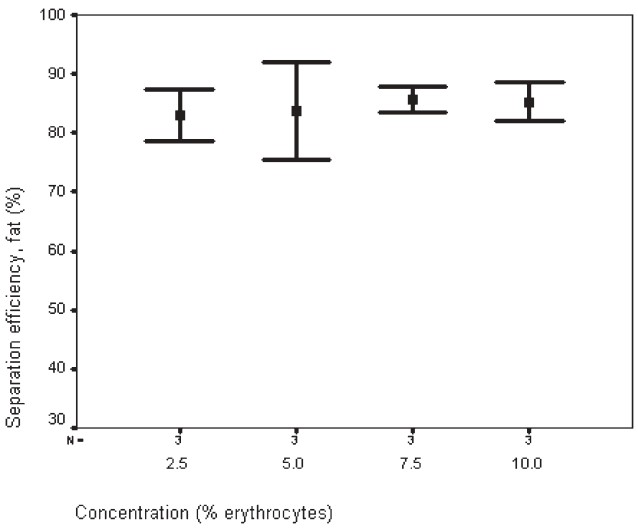

Fig. 17 Separation efficiency of lipid particles *versus* erythrocyte concentration (total flow rate: 0.3 ml/ min^{-1}, actuation frequency: $\sim$2 MHz, actuation voltage: 10 V_{pp}, lipid concentration: 1% by volume).

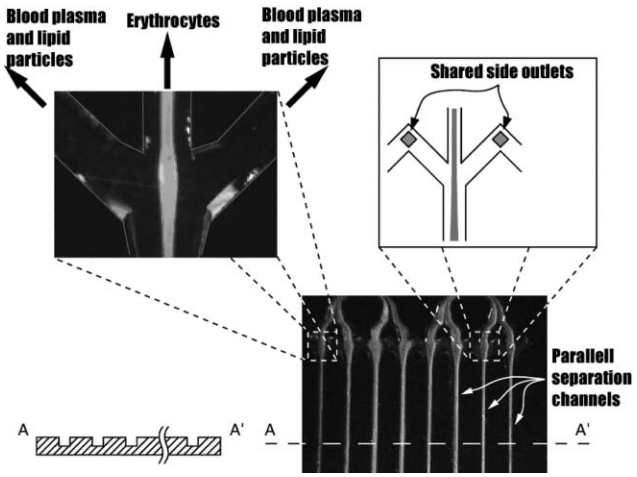

Fig. 18 Microscope images and illustrations of separation chip with eight parallel separation channels. The total flow rate during normal operation was in the 1 ml min^{-1} range.

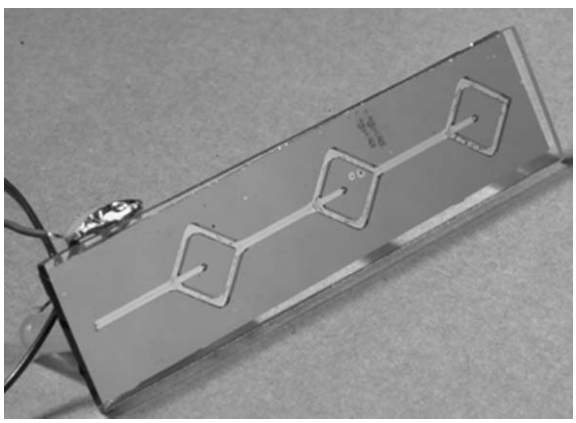

Fig. 19 Three-step serial separation chip for the separation of highly concentrated samples with minimal losses of the extracted particles.

shows the basic design of a chip for serial processing in three steps. The three centre outlets are enrichment outlets.

In addition to separating lipid particles from erythrocytes, the method has a clear potential in handling other blood component therapy tasks, *i.e.* it can be anticipated that the method can be further developed to enable separation of different blood cells and to produce clinically clean plasma.

The Lund method is a generic continuous-flow separation platform, offering low mechanical stress and non-contact processing of micrometer sized suspended particles. In theory, the only prerequisite is that the axial PRF is non zero, which is the case if the acoustic contrast factor is non-zero. By manipulating the density of the medium the contrast factor can be altered to some extent. Heating of temperature-sensitive samples due to losses in the piezo ceramic actuator and in the bulk material of the resonator can be avoided by cooling the chip, *e.g.* with a Peltier element.

A commonly raised issue in regards to cell handling in acoustic standing-wave fields is the potential harm that could be caused. In this respect viability studies supporting that ultrasonic manipulation of bioparticles is harmless have been performed by several researchers.[22,48,52] Thus, acoustic standing-wave technology seems to be a highly potent candidate for the development of new high performance platforms for manipulation and separation of cells. In the above described work performed on lipid microemboli separation from erythrocytes the degree of induced hemolysis was also investigated, showing that no significant increase in hemolysis could be detected after passing through the acoustic separator.[48] Also, unpublished results by M. Evander of the Lund-group, using the acoustic trapping device reported by Lilliehorn,[41] have recently shown that cells divide and proliferate in acoustic standing wave fields.

Aspects on system scaling

A generally raised concern regarding particle separation performed in microchip formats is the limited throughput of the systems presented. This is a fact that is inherently linked to the microscale environment in which the separation is performed. On the other hand, microscale is generally a prerequisite that offers the beneficial physical properties as such, where favourable scaling laws can be capitalized upon, *e.g.* laminar flow, which is a dominating flow regime in the microchip format. In regards to acoustic standing wave based particle separation, again, the scaling laws favour downscaling as the primary acoustic radiation force is directly proportional to the particle volume (radius to the 3rd power), which should enable the separation of similar particles sizes. Furthermore, the acoustic force on a particle is directly proportional to the employed frequency. Hence, as the dimension of the separation channel is reduced the fundamental resonance frequency is raised, suggesting that dimensions should be reduced when higher acoustic forces are sought. This in turn aligns well with efforts and needs in separation science for particle sizes ranging in the submicron range, 0.1–1.0 μm. It should also be acknowledged that as smaller particles are being processed the scaling laws strongly counteract favourable separation conditions due to the 3rd power dependency of the particle size for the PRF. This size domain is a very challenging area, where field flow fractionation,[53] FFF, currently is one of the dominating separation technology platforms, which yet requires a highly skilled approach for a successful outcome. Although far from proven, it can be hypothesized that acoustic separation may actually offer a viable way forward in the domain of nanoparticle separation. Along this line follows further dimensional reduction in order to match requirements on acoustic force in regards to the decreased particle size. Mixing effects due to induced acoustic streaming, which grows with reduced dimension, must also be suppressed along this development.

The benefits of microscale in regards to acoustic particle separation are evident and also fundamental to the separation performance. At the same time these facts clearly counteract the requirements on volumetric throughput of such systems. When designing systems for analytical purposes the actual miniaturisation is not really a problem in regards to throughput. On the other hand, a major part of the anticipated applications are seen in fields where a preparative scale is highly desired, as *e.g.* described in the cases of blood washing

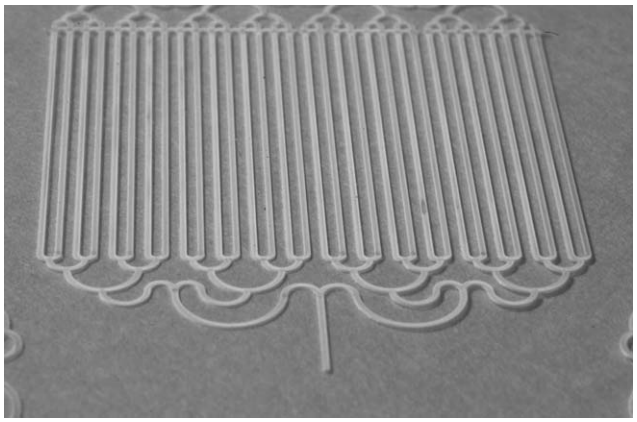

Fig. 20 2^5 bifurcation channel tree holding 32 parallel ~400 μm channels realised by micromilling in a polycarbonate sheet. It is possible to realize separation channels in polymers but due to acoustic losses in the bulk material this is less preferential.

in thoracic surgery or post surgery blood salvage. Clear areas are also seen in the blood banking units where blood component fractionation is a major task with throughput requirements of litres per hour or higher. An approach to meet these demands, which yet comply with the basic ideas of miniaturisation, is to implement a design that holds identical multiple parallel channels connected in a bifurcation structure such that the unit separation structure is simply replicated in a 2^n order, Fig. 20. Fig. 21 shows the layout of an eight-channel bifurcation erythrocyte extractor used in the thoracic surgery blood washing development,[48] where the inlet and outlet region of a silicon microdevice is seen in the SEM insert images.

A clear benefit of the transverse acoustic mode of operation described by the Lund group is the fact that the adaptation of the volumetric throughput can be done by increasing the number of parallel channels using the same piezoceramic actuator. Whereas the original single channel separator typically offered throughputs in the range of 100 μl min^{-1} the eight channel separator yielded flow rates in the order of 1 ml min^{-1}.

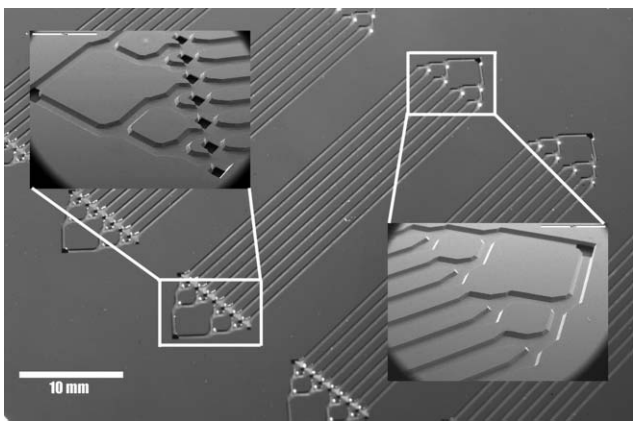

Fig. 21 Picture of eight channel separation structures with scanning electron micrographs showing details of the bifurcation channel outlets (left) and inlet (right). The row of black diamond-shaped structures are the waste outlets. These are connected to a common waste outlet on the back side of the chip. The single outlet at the far left is the enrichment outlet.

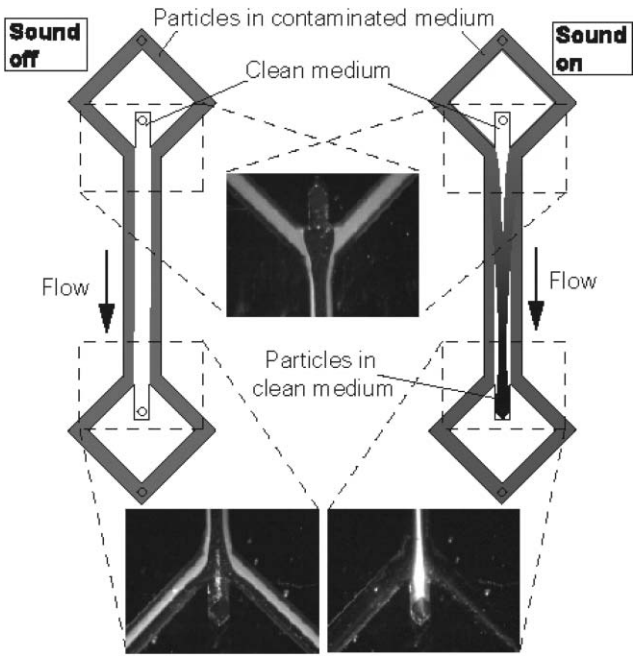

Fig. 22 Schematic illustration of the medium exchange principle with microscope images of the inlet and outlet channels. When the ultrasound is turned off the particles enter through the side inlets and exit through the side outlets together with the contaminated medium. If the ultrasound is turned on the particles are switched over to the clean medium and exit through the centre outlet.

Medium exchange through acoustic particle switching

Laminar flow microchannels offer the possibility to laminate different liquid media in a streaming system. This, combined with acoustic particle manipulation, can be utilized to move particles from one suspending medium to another by means of the axial PRF.[54,55] A particle suspension enters a rectangular cross-section microchannel, similar to the one used to separate lipid particles from erythrocytes,[46] through two side inlets (Fig. 22–24). A second, particle free, medium enters through a single centre inlet, whereby the centre fluid is laminated

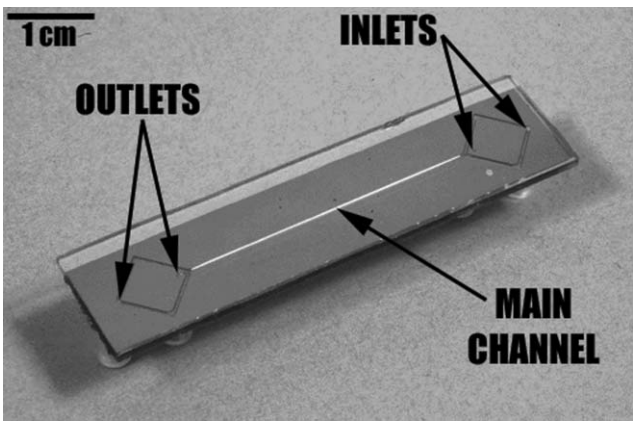

Fig. 23 Top view of the medium exchange chip.

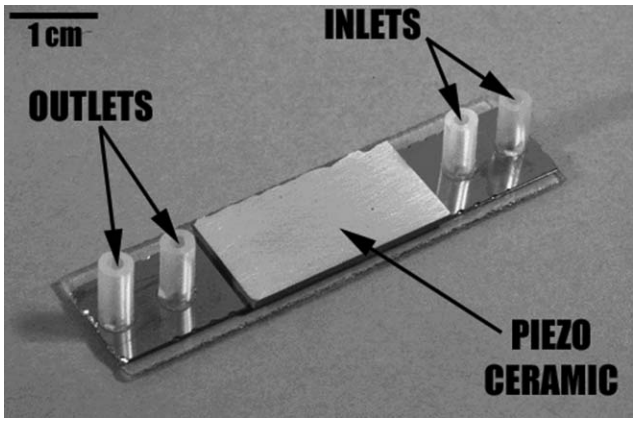

Fig. 24 Bottom view of the medium exchange chip with piezoelectric ceramic plate attached.

between the side inlet streams. If the particles have a positive ϕ-factor they will move from their original medium into the centre inlet stream, when a half wavelength standing wave is applied, and subsequently exit with the new medium through the centre outlet. This mode of operation can be used as a continuous particle washing system. The original medium exits *via* the two side outlets. Likewise, in cases where the particles have a negative ϕ-factor these are supplied *via* the centre inlet and are subsequently switched over to a clean medium entering through the side inlets.

When two media are laminated some lateral mixing will always occur due to diffusion. In the case of on-line particles washing, as described above in the medium exchange principle, diffusional mixing may induce undesired cross-contamination between the laminated streams. However, this problem can be eliminated by balancing the exit flow rates, ensuring that the diffusional mixing zone in the clear medium is directed to the waste outlet. When accounting for mixing effects, Rayleigh mixing[56] should also be considered. This becomes especially pronounced at low flow rate and high acoustic intensities and high frequencies. In separation systems where micrometer-sized particles are used and at the flow rates commonly used Reyleigh mixing can, in principle, be neglected.

The principle of medium exchange was demonstrated by translating 5 μm polyamide particles from a medium spiked with Evans blue to a clear medium. About 95% of the contaminant was removed (flow rate: 0.1 ml min^{-1} through side inlets and centre outlet and 0.17 ml min^{-1} through centre inlet and side outlets, actuation frequency: ~2 MHz, actuation voltage: 10 V_{pp}, particle concentration: 1.5% by volume, contaminant concentration: 360 μg ml^{-1}).[54] Similar medium exchange efficiencies were obtained when erythrocytes were translated from whole blood, spiked with Evans blue, to clean blood plasma. The balanced outlet flow eliminated diffusional cross-contamination and was an underlying reason to the high wash efficiency. It should, however, be noted that the medium exchange efficiency was found to decrease with increasing particle concentration. The sources of this contamination are assumed to be the hydrodynamic drag from each particle transiting the media boundaries and contaminants weakly adsorbed on the particle surfaces.

The described medium exchange method can be used to extend the applicability of the above described blood wash method to include post surgery blood recycling, *i.e.* when the patient is still bleeding in the post surgery intensive care and the shed blood is collected *via* a drain tube in the chest cavity. In this case the blood plasma can be heavily contaminated by drugs, immunologically active substances and coagulation factors that should not be returned to the patient. To avoid this, the erythrocytes can be moved from the contaminated plasma to clean plasma or saline solution for safe re-infusion.

Binary acoustic particle valving

The combination of the axial PRF and laminar flow micro-channels can also be employed to realize valve-less particle switches for controlled distribution of particles in microfluidic networks. Today, this is most commonly done through dielectrophoretic methods.[57] However, it is possible to apply the already described particle wash chips in binary switching networks. Unfortunately, that design does not allow this to be done in-plane with the microchip since the centre outlet must be connected to one of the succeeding inlets *via* an out-of-plane U-link. The design can, however, easily be modified to allow in-plane switching networks.[58] This is done by using only two inlets and two outlet channels (Fig. 25). Several of these switches can be interconnected in order to solve different particle distribution tasks. A four-outlet particle distribution chip design is described in Fig. 26 and the four binary settings of the chip in operation are shown. In this case transducer C1 was operated at ~1.9 MHz (~380 μm wide channel) and transducer C2 at ~1.6 MHz (~420 μm wide channel). The two operating frequencies were selected to avoid acoustic cross-talk between the two resonators. More complex particle handling tasks can be managed by integrating other

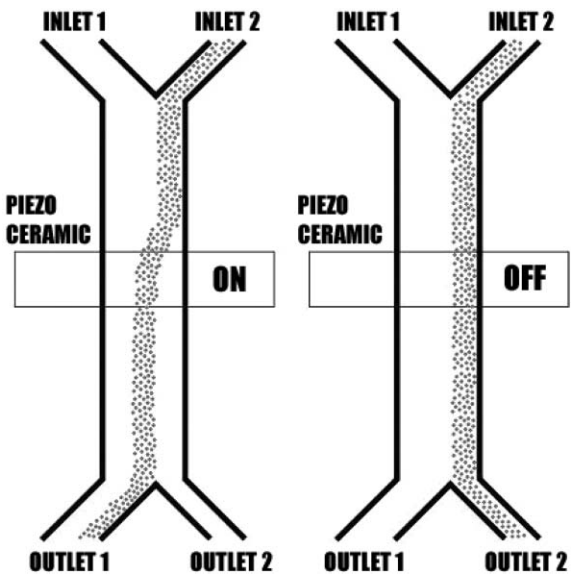

Fig. 25 Binary switching principle. Suspended particles enter through inlet 2 and a particle-free medium enters through inlet 1. By switching the piezoelectric ceramic on and off it can be decided whether the particles will exit through outlet 1 or 2.

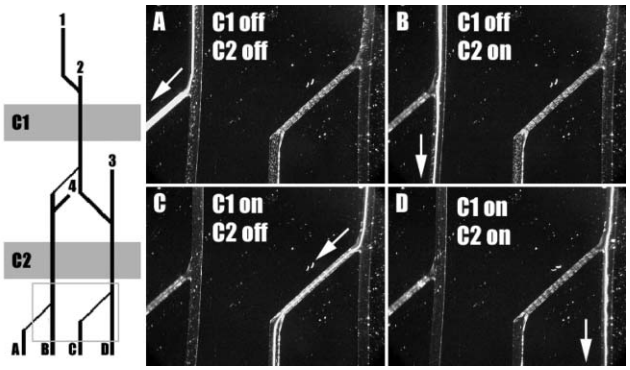

Fig. 26 Left: One possible design of a four-outlet binary switching tree. Suspended particles enter through inlet 1 while a particle-free medium enters through inlets 2, 3 and 4. By turning the piezo ceramics C1 and C2 on and off, in a binary code sequence, the particles can be directed to one of the four outlets A–D. Right: Microscope images of 5 μm polyamide particles exiting through one of the four outlet channels A–D. The field of vision corresponds to the grey square in the figure to the left.

components and procedures into the tree structure, *e.g.* acoustic particle traps[41] and medium exchange channels.[54]

For particle binary switching trees to reach their full potential some aspects must be accounted for. First of all, it is desirable to be able to operate the switches independently of the others. This can be done, as realised above, by operating the piezoelectric ceramic actuators at non interfering frequencies or by isolating them acoustically from each other. The latter can be done either by mounting several switching chips in a rig with interconnecting tubing or by attenuating the acoustic coupling between the actuators in the switching network. Secondly, the parabolic flow profile can cause problems when samples are transported through switching trees since particles travelling close to the top and bottom of the channel will travel slower than the ones in the centre. This can be addressed by applying a standing wave between the top and bottom of the channel, as well as between the channel side-walls, in order to keep the particles close together in the channel centre, thus reducing the particle velocity distributions. However, lagging particles will not be a problem if the sample volumes injected are small compared to the total volumetric flow rate and the number of consecutive switches is low.

The acoustic valving/binary switching concept inherently opens up an attractive area of automated on-chip particle sorting. The microfluidic system can be continuously inspected optically and thus a chip integrated rare event sorting/selection system can be realised. By defining an optical inspection point single particles with a characteristic optical property, *e.g.* a fluorescent label, can be selected from a dilute stream of particles by activating the channel acoustically as the fluorescent particle passes. This mode of operation has clear implications in cell sorting applications. When tailoring the acoustic valving concept to the selection and counting of cells, identified by fluorescently labelled cell-specific antibodies, an on-chip fluorescent activated cell sorting (FACS) system can be realised. In contrast to conventional FACS instrumentation cell/particle differentiation can in this case be implemented not

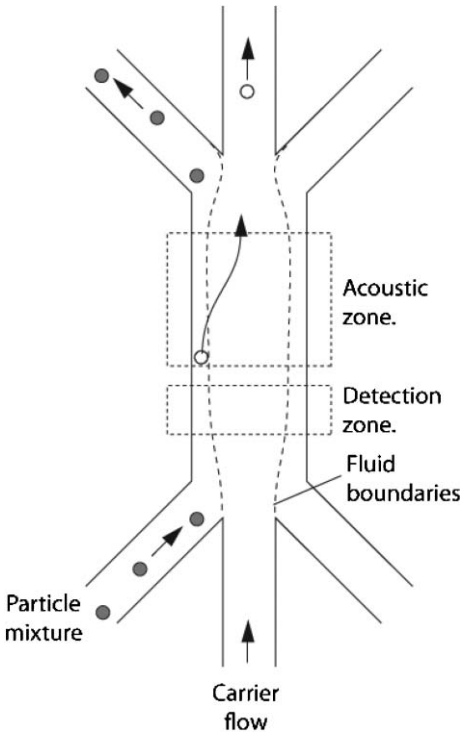

Fig. 27 Principle scheme for rare event particle sorting based on acoustic valving.

only based on fluorescently labelled entities but also with respect to the acousto-physical properties of the cells/particles. This may possibly hold promise of developing multiplex FACS-systems on chip that provide higher degrees of differentiation than current FACS-systems. Fig. 27 shows the principal operation of an optically triggered particle selection based on the acoustic valving principle. Fig. 28 indicates the power of the chip integrated format in the sense that high levels of multiplex particle/cell differentiation can be realised. A frequent argument with respect to chip based microfluidic FACS-systems is that the throughput is commonly orders of magnitude lower than which can be accomplished with conventional FACS-instrumentation. The acoustic valving approach, however, both displays a quite rapid acoustic switching of particles, typical transit time to the centre of a channel is in the order of 10–100 ms, and the fact that the concept is prone to massive parallelisation opens up the possibility to increase throughput by at least an order of magnitude.

Acoustic particle separation through frequency switching

By alternating between different channel resonance frequencies, matching the $n^*\lambda/2$ criteria, particles can be separated from each other.[59] This is made possible by the fact that the magnitude of the axial PRF differs between dissimilar particle types and spatial position in the standing-wave field. In the simplest case large and dense particles (positive ϕ-factor) are mixed with small and light (positive ϕ-factor) and enter the separation chip in Fig. 23 through the side inlets while a particle-free medium enters through the centre inlet. At time $T1$ (Fig. 29) a single wavelength standing wave (second harmonic, $\sim$4 MHz) is applied, thus the particles are gathered

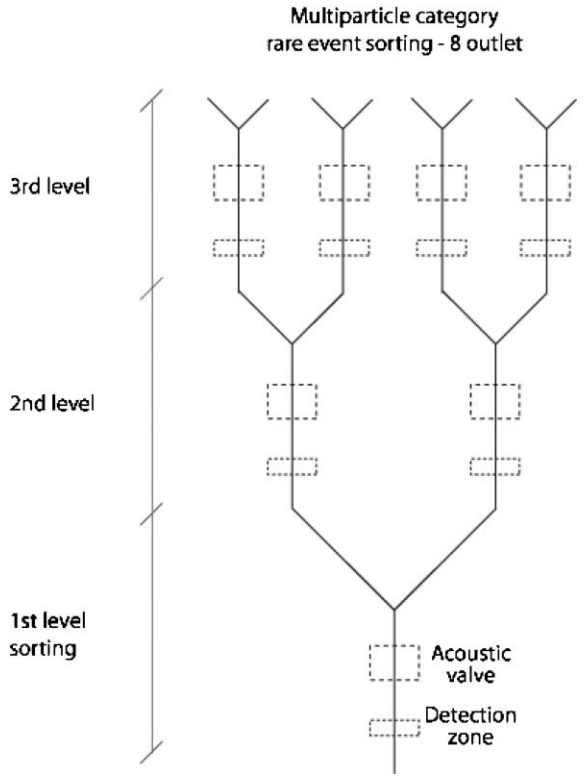

Fig. 28 Schematic layout for a 3 level acoustic valving set-up for multi-particle rare event sorting, having 8 outlet categories.

in the pressure nodal planes one quarter of the channel width from each side wall. When switching over to the fundamental resonance frequency (half wavelength, $\sim$2 MHz) the particles will start to migrate towards the pressure nodal plane in the centre of the channel ($T2$). The larger particles move faster because they are affected by a stronger axial PRF. If the frequency is switched back at the right moment the larger particles will be located close to the centre of the channel, where the axial PRF is at its minimum ($T3$). The smaller particles, on the other hand, will have moved only a small distance and, at time $T3$, start to move back to their position seen at time $T1$. After switching again ($T4$) the larger particles will be closer to the centre than at $T2$ while the smaller ones

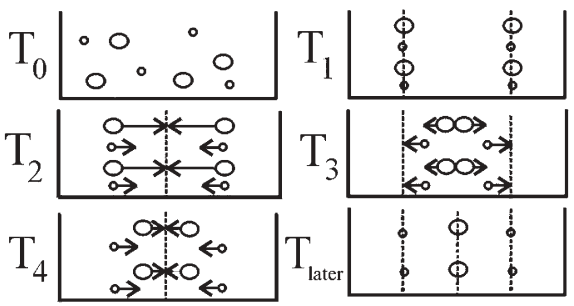

Fig. 29 Frequency switching separation principle. T_0 is the situation before the frequency switching starts. At T_1 and T_3 the frequency corresponds to the first harmonic of the channel (two pressure nodes). At T_2 and T_4 it corresponds to the fundamental resonance (one pressure node). When exiting the system the particles will have reached stable positions (T_{later}).

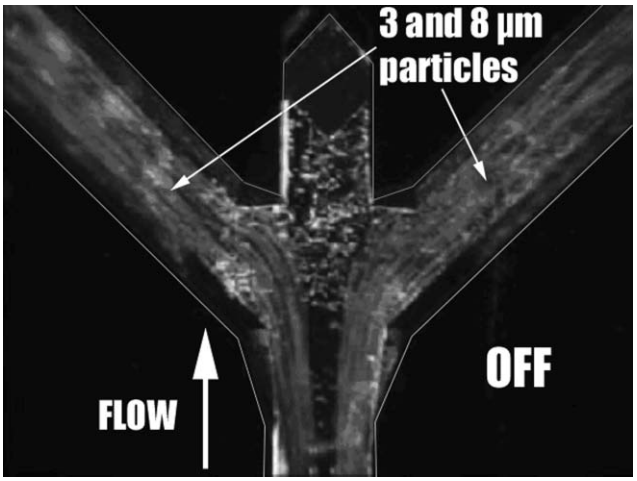

Fig. 30 Microscope image of the situation when the ultrasound is turned off. Both 3 µm and 8 µm particles exit through the side outlets.

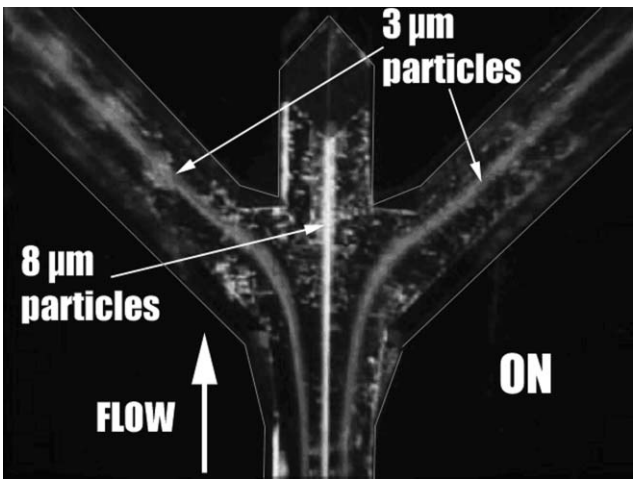

Fig. 31 Microscope image of the situation when the ultrasound is turned on. The 8 µm particles are focused in the fundamental resonance pressure node and exit through the centre outlet while the 3 µm particles are gathered in the first harmonic pressure nodes and exit through the side outlets.

will be at approximately the same position as at $T2$. If the switching continues the larger particles will end up in the middle of the channel and the smaller ones one quarter of the channel width from each side wall when they reach the outlets (Fig. 30 and 31). Using this method, it was demonstrated that at least 80% of the particles can be collected in the intended outlets when separating 3 µm polystyrene (1.05 g cm^{-13}) and 8 µm polymethylmethacrylate (1.22 g cm^{-3}) particles. The fundamental resonance and the second harmonic were typically active for 800 and 200 µs respectively (total flow rate: 90 µl min^{-1}).

Conclusions and outlook

The possibility to spatially control the positioning of particulate matter in continuously streaming microfluidic networks utilizing acoustic standing-wave forces opens the route to develop a whole set of new separation devices for

bioanalytical applications. The current review outlines several potential pathways for these developments, where *e.g.* differentiation of bioparticles that exhibit large differences in the acoustic contrast factor are easily separated as exemplified in the lipid microemboli separation from erythrocytes. On-line particle washing is also described as a possible way of performing continuous blood washing in situations where the blood plasma may be heavily contaminated by coagulation factors or inflammatory components. More intricate modes of operation are given in the acoustic binary valving concept for on-chip particle addressing, which also comprises the possibility of developing an acoustically controlled multiplex FACS-system. Furthermore, the new findings in acoustic frequency switching offer an electronically controlled mode of particle sizing which in a binary tree configuration could offer a system for continuous 2^n fraction particle size separation. Further developments based on continuous flow acoustic standing wave technology hold promise both of co-integration with elaborate lab-on-a-chip functionalities and interfacing to batch scale systems for analysis or meso scale preparative processing of bioparticulate matter.

Acknowledgements

The Swedish Research Council, Crafoordstiftelsen, Carl Trygger Foundation, Royal Physiographic Society in Lund, and Knut & Alice Wallenberg Foundation are greatly acknowledged for their financial support.

References

1 A. Kundt and O. Lehmann, *Ann. Phys. Chem.*, 1874, **153**, 1.
2 A. Nilsson, F. Petersson, H. W. Persson, H. Jönsson and T. Laurell, in *Micro Total Analysis Systems 2002*, Kluwer Academic Publishers, Nara, Japan, 2002, p. 751.
3 L. V. King, *Proc. R. Soc. London, Ser. A*, 1934, **A147**, 212–240.
4 K. Yosioka and Y. Kawasima, *Acustica*, 1955, **5**, 167.
5 L. P. Gorkov, *Sov. Phys. Dokl. (Engl. Transl.)*, 1962, **6**, 773.
6 W. L. Nyborg, *J. Acoust. Soc. Am.*, 1967, **42**, 947.
7 G. T. Haar and S. J. Wyard, *Ultrasound Med. Biol.*, 1978, **4**, 111.
8 T. Masudo and T. Okada, *Anal. Sci.*, 2001, **17**, 1341.
9 V. F. K. Bjerknes, in *Die Kraftfelder*, Braunschweig, Germany, 1909.
10 M. A. H. Weiser, R. E. Apfel and E. A. Neppiras, *Acustica*, 1984, **56**, 114.
11 L. A. Crum, *J. Acoust. Soc. Am.*, 1971, **50**, 157.
12 M. Groschl, *Acustica*, 1998, **84**, 432.
13 J. J. Hawkes, M. Gröschl, E. Benes, H. Nowotny and T. W. Coakley, *Proc. Forum Acusticum 2002 Sevilla*, Sevilla, Spain, September 16–20, 2002.
14 M. Hill, *J. Acoust. Soc. Am.*, 2003, **114**, 2654.
15 M. Hill, Y. J. Shen and J. J. Hawkes, *Ultrasonics*, 2002, **40**, 385.
16 M. S. Limaye, J. J. Hawkes and W. T. Coakley, *J. Microbiol. Methods*, 1996, **27**, 211.
17 C. M. Cousins, P. Holownia, J. J. Hawkes, M. S. Limaye, C. P. Price, P. J. Keay and W. T. Coakley, *Ultrasound Med. Biol.*, 2000, **26**, 881.
18 S. Peterson, G. Perkins and C. Baker, IEEE/Eighth Annual Conference of the Engineering in Medicine and Biology Society, 1986, p. 154.
19 J. J. Hawkes and W. T. Coakley, *Enzyme Microb. Technol.*, 1996, **19**, 57.
20 M. Groschl, W. Burger, B. Handl, O. Doblhoff-Dier, T. Gaida and C. Schmatz, *Acustica*, 1998, **84**, 815.
21 F. Trampler, S. A. Sonderhoff, P. W. S. Pui, D. G. Kilburn and J. M. Piret, *Bio-Technology*, 1994, **12**, 281.
22 P. W. S. Pui, F. Trampler, S. A. Sonderhoff, D. G. Kilburn and J. M. Piret, *Biotechnol. Prog.*, 1995, **11**, 146.
23 E. Benes, M. Groschl, H. Nowotny, F. Trampler, T. Keijzer, H. Bohm, S. Radel, L. Gherardini, J. J. Hawkes, R. Konig and C. Delouvroy, *Ultrasonics Symposium, 2001 IEEE*, 2001, **1**, 649.
24 H. Bohm, L. G. Briarty, K. C. Lowe, J. B. Power, E. Benes and M. R. Davey, *Biotechnol. Bioeng.*, 2003, **82**, 74.
25 S. Gupta and D. L. Feke, *Ultrasonics*, 1997, **35**, 131.
26 S. Gupta and D. L. Feke, *AIChE J.*, 1998, **44**, 1005.
27 M. T. Grossner, A. E. Penrod, J. M. Belovich and D. L. Feke, *Ultrasonics*, 2003, **41**, 65.
28 G. D. Pangu and D. L. Feke, *Chem. Eng. Sci.*, 2004, **59**, 3183.
29 M. Groschl, *Acustica*, 1998, **84**, 632.
30 J. J. Hawkes and W. T. Coakley, *Sens. Actuators, B*, 2001, **75**, 213.
31 K. Yasuda, S. Umemura and K. Takeda, *Jpn. J. Appl. Phys. Part 1*, 1995, **34**, 2715.
32 D. A. Johnson and D. L. Feke, *Sep. Technol.*, 1995, **5**, 251.
33 M. Kumar, D. L. Feke and J. M. Belovich, *Biotechnol. Bioeng.*, 2005, **89**, 129.
34 S. Kapishnikov, V. Kantsler and V. Steinberg, *Journal of Statistical Mechanics-Theory and Experiment*, 2006.
35 S. Gupta, D. L. Feke and I. Manas-Zloczower, *Chem. Eng. Sci.*, 1995, **50**, 3275.
36 Z. I. Mandralis and D. L. Feke, *AIChE J.*, 1993, **39**, 197.
37 A. Nilsson, F. Petersson, H. Jonsson and T. Laurell, *Lab Chip*, 2004, **4**, 131.
38 N. Harris, M. Hill, Y. Shen, R. J. Townsend, S. Beeby and N. White, *Ultrasonics*, 2004, **42**, 139.
39 N. R. Harris, M. Hill, S. Beeby, Y. Shen, N. M. White, J. J. Hawkes and W. T. Coakley, *Sens. Actuators, B*, 2003, **95**, 425.
40 M. Hill, J. J. Hawkes, N. R. Harris and M. B. McDonnell, *Proc. IEEE Sens. 2004, IEEE Int. Conf. Sens.*, 2004, 794.
41 T. Lilliehorn, U. Simu, M. Nilsson, M. Almqvist, T. Stepinski, T. Laurell, J. Nilsson and S. Johansson, *Ultrasonics*, 2005, **43**, 293.
42 T. Lilliehorn, M. Nilsson, U. Simu, S. Johansson, M. Almqvist, J. Nilsson and T. Laurell, *Sens. Actuators, B*, 2005, **106**, 851.
43 M. Wiklund, P. Spegel, S. Nilsson and H. M. Hertz, *Ultrasonics*, 2003, **41**, 329.
44 M. Wiklund, J. Toivonen, M. Tirri, P. Hanninen and H. M. Hertz, *J. Appl. Phys.*, 2004, **96**, 1242.
45 M. Elwenspoek and H. V. Jansen, *Silicon Micromachining*, Cambridge University Press, Cambridge, UK, 1998.
46 F. Petersson, A. Nilsson, C. Holm, H. Jonsson and T. Laurell, *Analyst*, 2004, **129**, 938.
47 S. M. Woodside, B. D. Bowen and J. M. Piret, *AIChE J.*, 1997, **43**, 1727.
48 H. Jonsson, C. Holm, A. Nilsson, F. Petersson, P. Johnsson and T. Laurell, *Ann. Thoracic Surgery*, 2004, **78**, 1572.
49 F. Petersson, A. Nilsson, C. Holm, H. Jönsson and T. Laurell, *Lab Chip*, 2005, **5**, 20.
50 D. M. Moody, W. R. Brown, V. R. Challa, D. A. Stump, D. M. Reboussin and C. Legault, *Ann. Thoracic Surgery*, 1995, **59**, 1304.
51 E. P. Mahanna, J. A. Blumenthal, W. D. White, N. D. Croughwell, C. P. Clancy, R. Smith and M. F. Newman, *Ann. Thoracic Surgery*, 1996, **61**, 1342.
52 D. Bazou, L. A. Kuznetsova and W. T. Coakley, *Ultrasound Med. Biol.*, 2005, **31**, 423.
53 J. C. Giddings, *Science*, 1993, **260**, 1456.
54 F. Petersson, A. Nilsson, H. Jonsson and T. Laurell, *Anal. Chem.*, 2005, **77**, 1216.
55 J. J. Hawkes, R. W. Barber, D. R. Emerson and W. T. Coakley, *Lab Chip*, 2004, **4**, 446.
56 M. Bengtsson and T. Laurell, *Anal. Bioanal. Chem.*, 2004, **378**, 1716.
57 T. Muller, G. Gradl, S. Howitz, S. Shirley, T. Schnelle and G. Fuhr, *Biosens. Bioelectron.*, 1999, **14**, 247.
58 M. Sundin, A. Nilsson, F. Petersson and T. Laurell, in *Micro Total Analysis Systems 2004, Malmö, Sweden*, Royal Society of Chemistry, Cambridge, UK, 2004, p. 662.
59 C. Siversson, F. Petersson, A. Nilsson and T. Laurell, in *Micro Total Analysis Systems 2004, Malmö, Sweden*, Royal Society of Chemistry, Cambridge, UK, 2004, p. 330.

